Preparation of Enzyme Crystals with Tunable Morphology in Membrane Crystallizers

Gianluca Di Profio,*,†,‡ Gisella Perrone,† Efrem Curcio,‡ Alberto Cassetta,§ Doriano Lamba,§ and Enrico Drioli†,‡

Institute on Membrane Technology (ITM-CNR), c/o University of Calabria, Via P. Bucci, CUBO 17/C, I-87030 Arcavacata di Rende (CS), Italy, University of Calabria, Department of Chemical Engineering and Materials, Via P. Bucci, CUBO 45/A, I-87030 Arcavacata di Rende (CS), Italy, and Institute of Crystallography (IC-CNR), Trieste Oustation, Area Science Park Basovizza, S.S. 14, Km. 163.5, I-34012 Trieste, Italy

Trypsins were crystallized by using membrane crystallization techniques, both in static and dynamic configurations. Crystal size distribution analysis revealed the high uniformity in size of the products that is achievable. Crystals produced by using membrane crystallization methods are more uniform than those obtained in conventional batch experiments. Crystals produced in forced solution flow are even more uniform than those obtained in a quiescent membrane system. Typical values obtained of percent standard deviation and Span are comparable to or even better than those reported in the literature. Crystal growth rate is favorably affected by solution convective motions in forced solution flow, by increasing solution velocity up to a maximum, which, in the best case, has been observed to be ca. 1500 μm/s. These high values of suitable velocities are characteristics of the membrane system; as with traditional method, growth rate deceleration was already visible at 250 μm/s. The maximum seems to be shifted according to the kinematic viscosity of the crystallizing solutions. Some crystals were assessed by X-ray crystallographic analysis, which demonstrated that dynamically grown crystals show no loss in diffraction quality with respect to static membrane crystallized proteins.

Introduction

Three-dimensional structure determination of proteins by X-ray diffraction analysis has lead in the past decades to essential contribution in fundamental understanding in biochemistry and biology.[1,2] Although nano-crystallogenesis is gaining increasing attention with the development of synchrotron microfocus techniques,[3,4] the crystallization step still remains the bottleneck for protein crystallography, since single and highly ordered crystals are required for structure determination at the atomic resolution level.[5] Indeed, biomacromolecules are rather reluctant to crystallize, because of their high level of structural complexity and their intrinsic evolutionary development toward the avoidance of aggregation in the living cell environment.[6]

On the other side, proteins, and more specifically enzymes, would have a wide range of applications in industry, thanks to their high substrate specificity.[7−9] In the past, their utilization in solution has been, however, rather limited due to some restrictions related to the intrinsic nature of these complex macromolecules, in conjunction with other limitations imposed by the media in which they are used: poor stability, variability of action, and/or high cost. Furthermore, proteins in crystalline formulation are characterized by pronounced fragility and dissolution or shattering under relatively mild conditions.

In this respect, among other methodologies aiming to obtain enzymes in stable formulations, the production of cross-linked enzyme crystals (CLECs)[10,11] is a simple, fast, and less expensive technique that does not require the utilization of chemical stabilizers, extreme temperature, and drying out steps[12] and that is opening important perspectives in the biotechnological field, such as in synthesis of fine chemicals, chiral intermediates, and peptides.[13−17] Despite the increased stability, the performance of CLECs depends on their structural and morphological characteristics, like polymorphism (when more than one polymorph can be grown), shape, size, and size distribution. These characteristics have a profound effect on the physical-chemistry parameters determining their efficacy, such as stability, melting point, dissolution rate, release of the activity, and so on. In each case, it is well-known that only crystals having uniform shape and size positively show their performances.[13,14] In this direction, new strategies and technologies addressed toward the production of crystals that are highly uniform in size and shape,[18,19] even on industrial-scale research of drug-active substances,[20] have recently been developed.

Membrane crystallization has been proposed as an interesting application of the membrane contactors technology[21] even for protein crystallization.[22−26] In a membrane crystallizer, a polymeric, microporous, and hydrophobic membrane is used as both (i) a physical support in order to separate two liquid subsystems and to accomplish the gas/liquid equilibrium and solvent removal in the vapor phase and (ii) the active medium for the primer of the heterogeneous crystallization step. The driving force for the process is supplied by a vapor pressure difference on both sides of the membrane,

* To whom correspondence should be addressed. Tel.: +39 0984 492014. Fax: +39 0984 402103. E-mail: g.diprofio@itm.cnr.it.

† Institute on Membrane Technology (ITM-CNR), c/o University of Calabria.

‡ University of Calabria, Department of Chemical Engineering and Materials.

§ Institute of Crystallography (IC-CNR).

10.1021/ie0508233 CCC: $30.25
Published on Web 11/08/2005

generated by the difference in solute concentration, while the hydrophobic nature of the membrane prevents the mass transport in the liquid phase. Membrane crystallization of proteins can be accomplished both in static and forced solution flow configurations. In the last case, the axial flow in the laminar regime is expected to stabilize the crystal growth process, thus producing crystals with improved structural features. Enhanced crystallization kinetics has been recognized as the main feature of this technique, both in forced solution flow and static conditions.[24,26]

In the present work, enzymes belonging to the family of serine proteases, namely bovine and porcine pancreas trypsins, have been crystallized by using membrane crystallization techniques both in static (quiescent) and dynamic (forced solution flow) configurations. The crystals obtained have been subjected to morphological and structural characterization by X-ray crystallographic analysis in order to clarify the potentiality of the membrane-based techniques for producing highly uniform-size crystals, with "tunable" morphologies, preserving high structural order and diffracting power. The outcome of the main fluidynamic parameter affecting the crystallization kinetics, i.e., the solution velocity in forced solution flow system, was investigated and related to the yield of the crystallization process.

Moreover, efforts addressed to clarify the effect of the solution convective motions on the crystal growth process have also been the object of the present study. In fact, several attempts have been pursued in the past in order to clarify the effect of the forced solution flow on the protein crystallization process. An old belief is that flow affects the crystallization process in a detrimental way.[27−30] Crystallization in a microgravity environment in some cases supported this hypothesis.[31] In some other cases, instead, no effect of solution flow was visible.[32] More recently, completely opposite evidence has been observed in several experimental and theoretical studies,[33−36] and a more reliable explanation has been proposed by some authors supporting the idea that macromolecular crystallization in conditions of axial flow in the laminar regime will improve the crystallization process, thus leading to high-quality crystals. [22]

In the crystallization process, the growth can be governed either by a transport and/or by a kinetic control mechanism. In the first case, the crystal growth rate depends on the rate for the solute molecules to be supplied to the growing surface from the bulk of the solution; since convection will increase the rate of solute supply, it is expected that increasing solution velocity will increase crystal growth rate. In the second case, growth rate is governed by the rate of the molecules to be included on the growing face from the interface solid/solution; in these conditions, it has been observed that flow does not affect the interfacial kinetics of solute incorporation into the crystals.[37] Under static conditions, the growth mechanism has been described to be a combination of both surface kinetics and bulk-transport-based control. In this case, intrinsic instability of the growth process leads to a fluctuation in growth rate, step density, and step velocity (ca. 80% of their respective average values), thus inducing a decrease in the homogeneity of the crystals, with the appearance of striae on the crystal surface.[38] The strongest instability is expected for processes that operate under equal influence of the transport and kinetics components on the overall control rate.[38] Then, the shift of the working conditions to pure kinetic or transport control mechanism, starting from a mixed condition (static), by, for example, forced solution flow, should result in a more steady growth, thus obtaining higher crystal quality. X-ray diffraction analysis carried out on crystals grown in not-steady conditions seems to support this assumptions.[34,35]

For these reasons, trypsin crystals grown by membrane crystallization in forced solution flow regime have been analyzed by X-ray diffraction at the Italian synchrotron light laboratory Elettra, Trieste (Italy). Structural features have, thus, been compared with those exhibited by crystals obtained in a static membrane system.

Experimental Section

Lyophilized bovine pancreas (BPT) and porcine pancreas (PPT) trypsins (MW $\approx$ 23 800 g mol^{-1}) were used as purchased (Sigma-Aldrich) without any further purification. BPT crystallizing solutions were prepared by mixing equal volumes of the protein solutions (containing BPT 30 mg/mL, Benzamidine hydrochloride 10 mg/mL, and $CaCl_2$ 6 mM) with ammonium sulfate or polyethyleneglycol (PEG, MW $\approx$ 6 000 g/mol), dissolved in TRIS−HCl buffer, 0.1 M, pH 8.5. In the same way, PPT 40 mg/mL, dissolved in a $CaCl_2$ 6 mM solution, was mixed in a 1:1 volume ratio with ammonium sulfate, dissolved in TRIS−HCl buffer solution, 0.1 M, pH 8.5. All the solutions were prepared in bidistilled water. Finally, 3 mL of crystallizing solutions were used for each dynamic experiment and 1.2 mL for the static ones. The final solutions were 0.22 μm filtered by syringe filters before the crystallization runs.

Hydrophobic, polypropylene hollow fibers membranes (Accurel PP, nominal pore size of 0.2 μm, from Membrana GmbH, Germany), were used in all the experiments. Aqueous solutions of calcium chloride, 25% w/v, were used as the stripping agent. All the experiments were carried out at 20 °C.

Experiments were conducted in a static and dynamic membrane crystallizer apparatus by using the configurations described elsewhere.[24,25] Tests were carried out in static configurations by changing the active membrane surface and flow rate of solvent extraction from the protein solutions toward the stripping side, while in dynamic configurations they were performed by varying the crystallizing solution velocity (v). Control experiments were done in batch mode, using the same initial conditions of supersaturation but without using membrane fibers, both for BPT and PPT systems.

Microscopic observations, by an optical microscope (ZEISS-Axiovert 25, equipped with a video camera), were performed every 24 h for a week after the appearance of the first visible crystals; pictures were recorded for evaluating the progress of crystal size distributions (CSDs), both for crystal length (l) and width (w) (as defined in ref 24), as a function of time, to determine the crystal growth rate (G). Depending on the homogeneity of the samples, assessed by optical inspection before image collections, 150−300 crystals were analyzed for each CSD.

Membrane performances have been determined by measuring the rates of solvent extraction, while observing the volume reduction factor of pure water throughout, on the one side of the membrane fibers, under the effect of the same stripping solution used during the

crystallization trials. Kinematic viscosity for the various solutions has been measured by Ubbelohde capillary viscosimeters (from Bicasa, Italy).

The apparent percent yield of the crystallization experiments for PPT was calculated by measuring the protein concentration in the solution, by standard spectrophotometer procedure, before the crystallization tests and in the supernatant after each experiment. To ensure that none of the crystals were left in solution, the supernatant was filtered by a syringe filter (0.22 μm) and then diluted to a known volume with the same buffer used in the experiments. The absorbance was measured at 280 nm by a UV-spectrophotometer (Shimadzu UV-160 recording spectrophotometer).

Results and Discussion

Effect of the Forced Solution Convection on the Crystal Growth Kinetics. Figure 1 shows the graphs of the crystal length and width growth rate (G_l and G_w) as a function of the recirculating solution velocity (v) for BPT crystallized with PEG 6000 (BPTPEG) and PPT crystallized with ammonium sulfate (PPTAS); their behaviors have the typical bell shape reported in previous papers.[25,26,33] The same curves obtained for BPT crystallized with ammonium sulfate[25] (BPTAS) are also reported in the figure. In the latter two cases, the maximum values for G_l and G_w are reached for the same v of 895 μm/s and 932 μm/s for BPTAS and PPTAS, respectively. When BPT is crystallized with PEG 6000, the maximum for G_l is shifted up to $v = 1498$ μm/s, while the G_w maximum is at about $v = 1116$ μm/s.

Attempts to elucidate the dependence of G on the solution convective motions have been discussed in recent papers. Vekilov and Rosenberger[33] reported the increase in the average growth rate by increasing v up to 250 μm/s, for high-purity hen egg white lysozyme (HEWL) solutions crystallized in forced solution flow configuration, with the enhancement in the convective supply of the growing units to the solid/liquid interface. For higher v values, the observed growth rate deceleration, up to growth cessation, has been attributed to the overpowering of the convection-enhanced supply of impurities that are incorporated into the crystal in an impeding manner for the growth kinetics. These descriptions seem to be supported by the fact that, even by using high-purity solutions, $v > 250$ μm/s led to growth deceleration, and with less-pure protein solutions, growth deceleration occurred at any $v > 0$. Similar dependence of G from v has been observed for HEWL[26] and bovine trypsin[25] crystallized in a forced solution flow membrane crystallization apparatus. This behavior has been explained by a shifting of the operative system working point to a regime with significantly faster transport and higher relative weight of interfacial kinetics effects in the overall control of the crystallization process. Peclet number calculations confirmed this shifting.[26] Namely, the increase in v induced a decrease in the boundary layer thickness (δ, proportional to $v^{-1/2}$), thus resulting in a decrease of the Peclet number, with the consequent switch from diffusive to interfacial kinetics of the overall mass-transfer process control.[37]

However, δ is also proportional to the kinematic viscosity ($v^{1/6}$) of the solution,[39] so that the increase in v would allow one to shift the maximum observed in the G vs v plots toward higher values of v for solutions with an increased kinematic viscosity. In ref 26, the maximum of the curve falls at $v = 1100$ μm/s for HEWL,

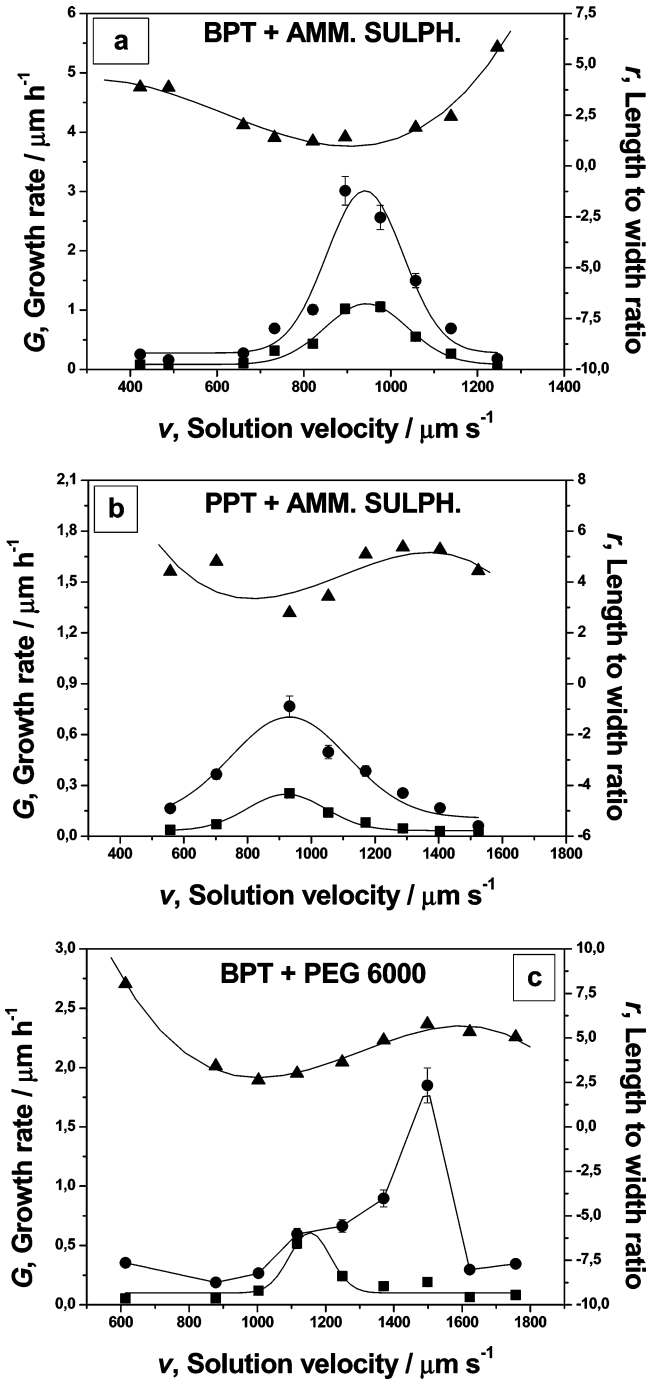

Figure 1. Crystal width G_w (■) and length G_l (●) growth rate and length-to-width ratio r (▲) as a function of the macromolecular solution velocity (v), for the three protein systems investigated in dynamic configurations: (a) BPT + ammonium sulfate; (b) PPT + ammonium sulfate; and (c) BPT + PEG 6000 (solid lines represent just a guide for the reader).

assuming v of 1.4×10^{-2} cm^2/s. Here, the measured values of kinematic viscosity for the three trypsin solutions are as follows: $v_{BPTPEG} = 1.92 \times 10^{-2}$ cm^2/s; $v_{PPTAS} = 0.82 \times 10^{-2}$ cm^2/s; $v_{BPTAS} = 0.79 \times 10^{-2}$ cm^2/s. These values seem to reflect the order of the maximum of the G_l and G_w curves for the three systems BPTPEG > HEWL[26] > PPTAS $\approx$ BPTAS, which still supports the proposed mechanism.

A controversial point, however, relies on the decrease of G values by increasing v after reaching the maximum. Although some impurity effects were detected and estimated by Curcio et al.,[26] experimental evidence of

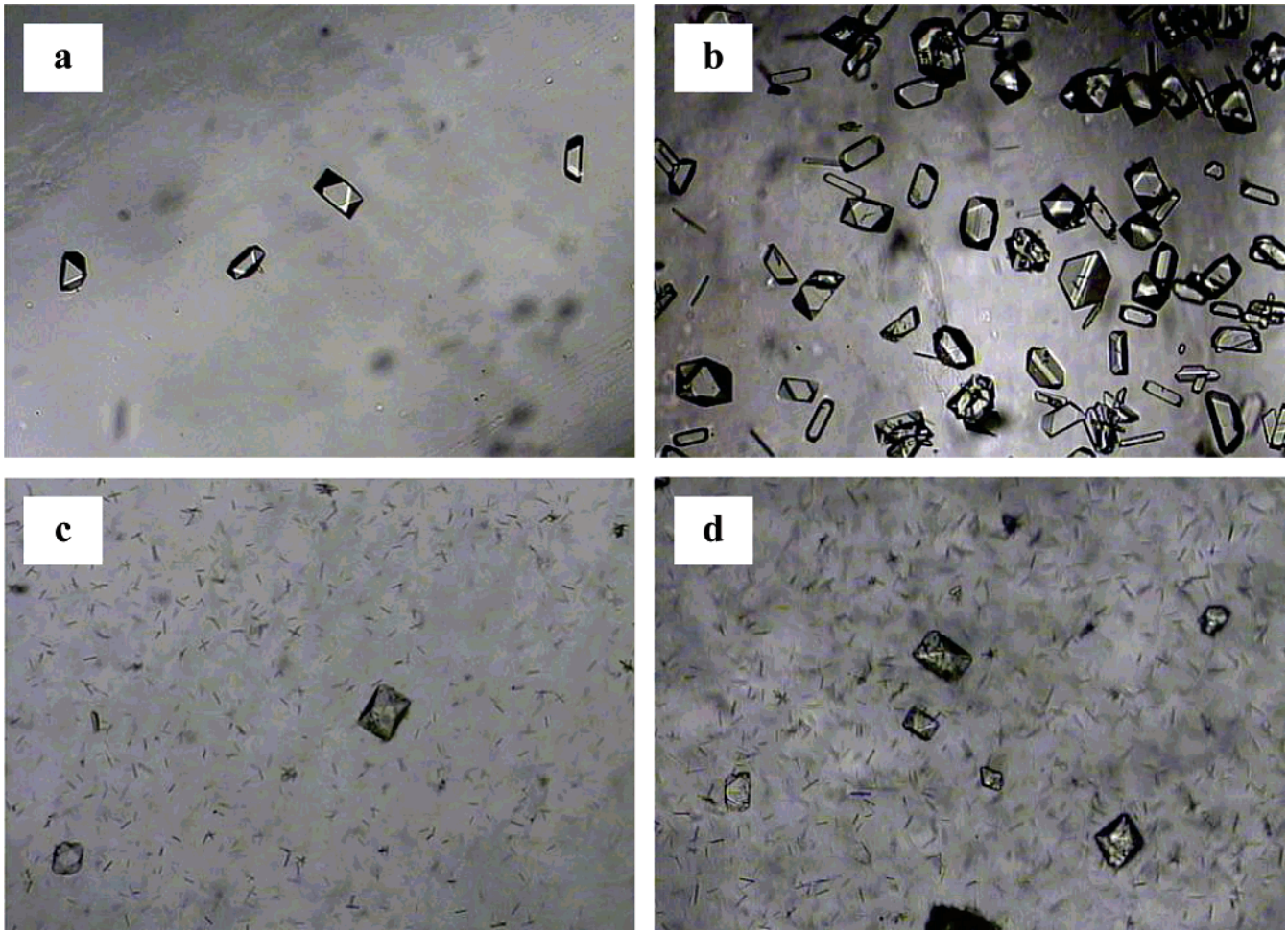

Figure 2. BPT crystals obtained in forced solution flow configuration with ammonium sulfate as precipitant, at: (a) 423 μm/s; (b) 821 μm/s; (c) 1072 μm/s; and (d) 1139 μm/s of recirculating solution velocity.

excess nucleation has been observed for v values after the maximum of the curves in the membrane system (ref 26 and in the present work). Moreover, in view of the low-purity level of the protein solutions that have been used in these experiments,[25,26] this suggests that the effect of impurities only partially could be ascribed to the crystal growth rate deceleration in the membrane-based techniques for high v values, but it is mainly due to the excess of nucleation. A possible explanation could be in accordance with the hypothesis[40] that high protein concentrations in the boundary layer close to the solid/liquid interface, which is actually the case of a kinetic control-based mechanism, might lead to secondary nucleation, which in turn gives rise to excess nucleation and, therefore, to a crystal shower that suppresses growth. Figure 2, parts c and d, shows this phenomenon, where big crystals are surrounded by a huge amount of smaller tiny crystals that, in the hypothesis sustained, are generated by secondary nucleation in the boundary layer at the solid/liquid interface.

Interestingly, while for BPTAS and PPTAS both G_l and G_w reach their maximum values ~900 μm/s, for BPTPEG the maximum is shifted to $v = 1116$ μm/s for G_w and to 1498 μm/s for G_l. This could be ascribed mainly to the orientation of the growing crystals in the direction of the convective flow,[26] because of the redirection of their Brownian motion by the forced convective motion, which affects the growth rate of the different crystal faces in a different manner.

While for less viscous solutions this induces no variations in the maximum values of G_l and G_w (Figure 1 parts a and b), when the viscosity of the solution increases up to 1.92×10^{-2} cm^2/s, the splitting between the two maximums for G_l and G_w becomes well visible (Figure 1c).

Trypsin crystals obtained by using the static and dynamic membrane crystallization setup have been investigated by means of single crystal X-ray diffraction using synchrotron radiation at the Italian synchrotron light laboratory Elettra, Trieste (Italy). A detailed crystallographic analysis including data collection and processing statistics, phasing, and crystallographic refinement will be published elsewhere. The electron density maps calculated at the final stage of the crystallographic refinement (see Figure 3) are a good indicator of the high quality of the trypsin crystals obtained by either of the two membrane-based crystallization methodologies. This demonstrates that good diffracting-power enzyme crystals, potentially useful for X-ray crystallography studies, can be produced by the system.

Crystal Morphology. It has been noted that uniform-shaped trypsin crystals, with narrow size distribution, can be obtained by using a membrane crystallization technique, according to the experimental running conditions.[25] In the present study, to quantify and compare the narrowness of the CSDs with literature data, the variation coefficients (CV) and the Span, as defined by eqs 1 and 2, have been computed by using the crystals'

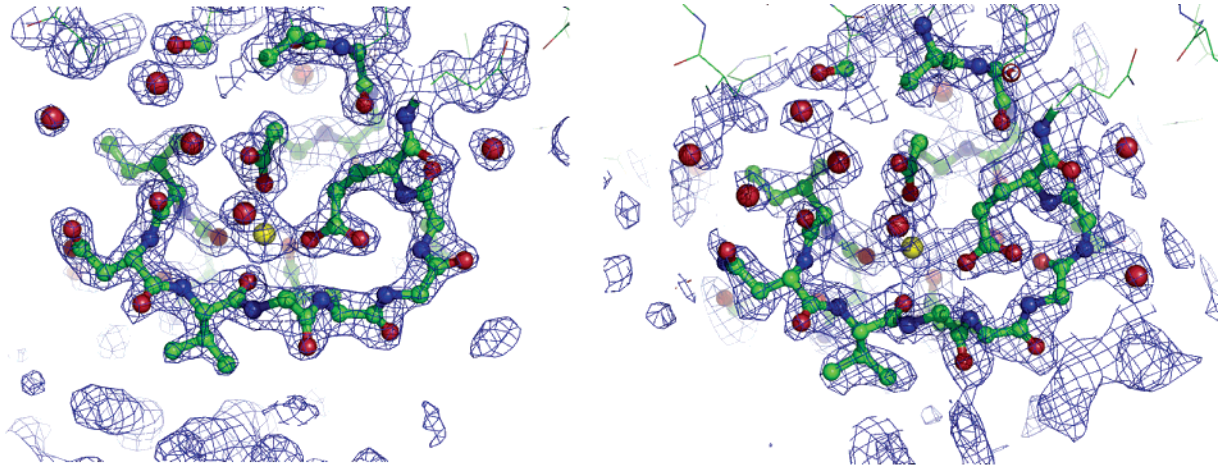

Figure 3. A portion of the $2m|F_o| - D|F_c|$ σ_a weighted density map (1.0σ cutoff) around the calcium binding site in porcine trypsin. (a) PPTAS, static setup with 6 membranes; cell dimensions, a = 47.03, b =54.16, c = 77.66 Å; space group = $P2_12_12_1$; resolution = 1.90 Å). (b) bovine trypsin (BPTAS, dynamic setup v = 821 μm/s; cell dimensions, a = 62.91, b = 63.28, c = 68.57 Å; space group = $P2_12_12_1$; resolution = 2.00 Å. The figure has been prepared with PYMOL (http://www.pymol.org).

length and width CSD values for each of the three protein systems examined.

The variation coefficient is defined by

$$\mathrm{CV} = \frac{d_{80\%} - d_{20\%}}{2d_{50\%}} \tag{1}$$

The Span of the distribution has been calculated as

$$\mathrm{Span} = \frac{d_{90\%} - d_{10\%}}{d_{50\%}} \tag{2}$$

In the above equations, d is the size smaller than or equal to that for the $xx\%$ amount of the considered particle population. Percent standard deviation ($\sigma\%$) has been calculated by dividing the standard deviation by the average crystal size.

In Tables 1 and 2 are reported the average crystal size (length and width), the percent standard deviation, the variation coefficient, and the Span for the three crystallizing systems considered. Overall, in the dynamic case, very low values of CV and Span are observed for trypsin crystals both for l and w, depending on the operative conditions. The average values for the variation coefficient are <25% for w and nearly 30% for l. Considering that values of CV ~50% are typical in large-scale crystallization processes, the results observed assume particular interest from the standpoint of a pharmaceutical company, since crystals with controlled shape and uniform size are highly required. For instance, pharmaceutical active molecules such as 3-ketodesogestrel (MW 433.50 g mol^{-1}) and progesterone (MW 314.45 g mol^{-1}), which are rather less complex molecular systems than trypsin, were recently crystallized by using a novel membrane-based anti-solvent solidification technique.[20] A high level of uniformity has been depicted by the authors for the crystals produced with this technique, as demonstrated by measuring (by laser diffraction methods) values of Span in the range of 1.6 and 3 for 3-ketodesogestrel and 1.7 and 2 for progesterone, depending on the specific operative conditions. This is remarkable considering that Span values <1.4 are considered to be exceptional for a solidification process such as crystallization.[20] In the present study,

Table 1. Average Width (w), Percent Standard Deviation ($\sigma\%$), Variation Coefficient (CV), and Span as a Function of the Solution Velocity (v), in Dynamic Conditions, and the Number of Fibers Inside the Module (m), in Static Configuration, for the Three Trypsin Systems Studied in This Work[a]

v (μm s^{-1})	w (μm)	σ (%)	CV	Span	m (no.)	w (μm)	σ (%)	CV	Span
BPT + ammonium sulfate									
488	10.1	0.588	0.187	0.499	1	35.6	0.394	0.389	2.111
661	22.7	0.688	0.249	1.375	2	32.9	0.379	0.375	1.917
732	30.3	0.093	0.249	0.875	3	30.5	0.375	0.188	1.875
821	70.7	0.530	0.329	1.260	4	21.5	0.319	0.214	1.714
976	41.3	0.148	0.389	1.222	5	21.5	0.304	0.182	1.637
1072	24.9	0.081	0.187	0.625	6	19.7	0.214	0.188	1.728
1139	18.6	0.886	0.199	0.899	batch	51.2	0.552	0.480	2.434
BPT + PEG 6000									
613	8.7	0.202	0.187	0.500	1	39.5	0.389	0.318	2.059
879	9.6	0.226	0.167	0.556	2	32.2	0.576	0.346	1.941
1116	18.9	0.256	0.300	1.100	3	30.1	0.385	0.365	1.750
1249	14.5	0.322	0.350	1.200	4	28.2	0.302	0.250	1.650
1370	12.1	0.405	0.250	0.999	5	28.0	0.439	0.292	1.556
1498	11.4	0.269	0.250	0.750	6	13.2	0.314	0.333	1.154
1757	8.7	0.456	0.333	1.000	batch	35.8	0.526	0.455	2.24
PPT + ammonium sulfate									
557	7.5	0.167	0.125	0.375	1	29.5	0.551	0.433	1.895
702	10.2	0.278	0.208	0.599	2	25.8	0.445	0.389	2.222
932	15.7	0.210	0.214	0.615	3	28.9	0.396	0.361	1.491
1053	11.3	0.185	0.227	0.444	4	16.8	0.349	0.353	1.089
1287	6.9	0.344	0.214	0.556	5	19.8	0.260	0.222	0.838
1404	7.3	0.549	0.199	0.778	6	11.6	0.227	0.25	0.611
1524	7.8	0.259	0.187	0.625	batch	34.7	0.510	0.604	1.999

Span was calculated for the trypsin crystal populations directly from the CSDs, according to eq 2. In the majority of the experiments, Span is consistently <1; only in a few cases it is slightly >1. The highest value measured was 1.7 for l. PPT crystals were usually more uniform than BPT ones, regardless of the precipitant being used.

The values of $\sigma\%$ are even reported in Tables 1 and 2. Falkner et al.[18] measured very low values of $\sigma\%$ (~10% in the most favorable conditions) when lysozyme was crystallized in a region of its phase diagram where the protein solubility is very low, thus producing a large amount of small nuclei. The values of $\sigma\%$ obtained for trypsin well approach the values reported. In the most favorable cases, $\sigma\%$ has been measured to be 8.1% and 9.3% for BPTAS crystals width. The point of interest

Table 2. Average Length (l), Percent Standard Deviation (σ%), Variation Coefficient (CV), and Span as a Function of the Solution Velocity (v), in Dynamic Conditions, and the Number of Fibers Inside the Module (m), in Static Configuration, for the Three Trypsin Systems Studied in This Work[a]

v (μm s^{-1})	l (μm)	σ (%)	CV	Span	m (no.)	l (μm)	σ (%)	CV	Span
BPT + ammonium sulfate									
488	41.8	0.319	0.241	0.793	1	103.8	0.631	0.695	1.538
661	59.0	0.618	0.487	1.257	2	82.4	0.581	0.513	1.643
732	77.9	0.703	0.269	0.923	3	75.1	0.338	0.387	1.645
821	93.4	0.635	0.360	1.000	4	59.7	0.267	0.362	1.216
976	46.8	0.177	0.294	1.118	5	63.9	0.276	0.365	0.806
1072	40.3	0.128	0.208	0.667	6	76.4	0.179	0.192	0.938
1139	32.3	0.145	0.299	1.000	batch	147.3	0.763	0.521	1.981
BPT + PEG 6000									
613	74.4	0.346	0.479	1.312	1	116.0	0.537	0.432	1.833
879	34.4	0.317	0.258	0.729	2	71.1	0.546	0.463	1.630
1116	45.2	0.397	0.216	0.783	3	55.9	0.404	0.409	1.846
1249	54.3	0.489	0.329	0.982	4	57.6	0.434	0.353	1.528
1370	69.6	0.342	0.349	1.107	5	54.4	0.382	0.314	1.220
1498	92.4	0.191	0.265	0.925	6	47.6	0.352	0.216	1.244
1757	39.3	0.482	0.296	1.137	batch	85.1	0.677	0.558	2.059
PPT + ammonium sulfate									
557	29.6	0.182	0.167	0.481	1	99.1	0.533	0.574	1.886
702	41.8	0.409	0.311	0.889	2	84.4	0.561	0.509	1.327
932	50.8	0.252	0.270	0.784	3	52.8	0.379	0.363	1.394
1053	46.7	0.147	0.200	0.640	4	61.1	0.367	0.286	0.863
1287	33.0	0.284	0.250	0.727	5	45.6	0.292	0.269	0.714
1404	30.3	0.565	0.318	0.909	6	50.0	0.229	0.250	0.609
1524	32.6	0.369	0.290	0.935	batch	123.2	0.794	0.568	2.415

[a] Measurements carried out at ~24 h since the appearance of the first visible crystals.

is, however, that the high uniformity in crystal size has been kept even when big crystals were produced, on what concerns both crystals' width and length size. Taking into account the values of the statistical parameters used to evaluate the degree of uniformity of the membrane-based crystallized proteins, with respect to other high efficient strategies/techniques recently explored, the advantage of the membrane crystallization method appears evident.

As matter of comparison, Tables 1 and 2 report the values of CV and Span for BPT and PPT crystals obtained by the static membrane crystallization system and by batch crystallization. Batch crystals are always less uniform in size than membrane-crystallized ones. Trypsin crystals produced in forced solution flow configuration at values of solution velocities around the maximum of the G_l and G_w values vs v show comparable values of CV and Span to those obtained in the static membrane crystallization tests. For v values above and below the maximum, narrower CSDs were measured. An increase of CV has been, however, observed for extreme values of v, in those regions where an excess of nucleation is observed in the system. This is still in accordance with the hypothesis of the secondary nucleation for extreme v, so that the existence of two populations of crystal size will lead, in some extent, to a lower level of uniformity in the CSD. Nevertheless, the lower number of big crystal surrounded by a huge amount of smaller ones (Figure 2 parts c and d), has induced a detrimental effect on the overall uniformity of the product only to a minor extent, as the CSDs were determined on the number of the crystals.

The ratio l/w, indicated as aspect ratio (r), has been even reported as a function of the solution velocity in Figure 1. The most interesting remark is that, in every case, the aspect ratio has been controlled by acting on the recirculation solution velocity, thus producing crystals with a "tuned" shape.

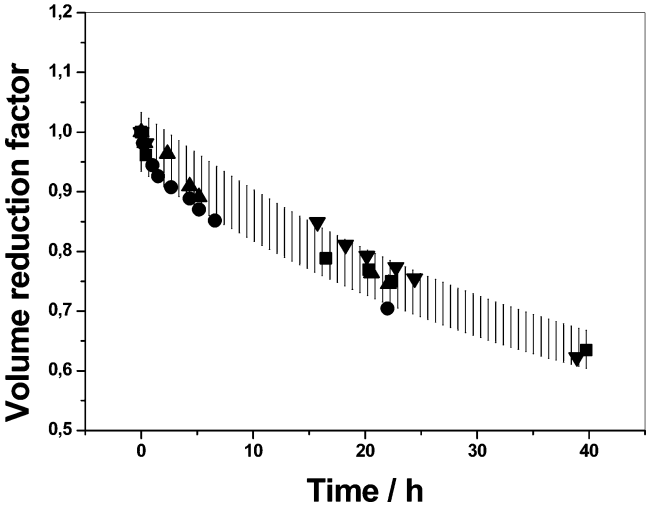

Figure 4. Volume reduction in the time for pure water (on the protein side) extraction by the same stripping solution used in the crystallization experiments for PPTAS. Measurements have been performed: ■ before the experiments; ● after the crystallization test operated at v = 932 μm/s; ▲ after the crystallization test operated at v = 1171 μm/s; and ▼ after the crystallization test operated at v = 1404 μm/s. Vertical bars indicate the variation within the 5% with respect to the average values of the best fitting curves (not showed).

Membrane Performances. A crucial point regarding a possible application of the membrane-based method in a large-scale crystallization setup relies on the membrane performances. In principle, although generally controllable, membranes are subject to fouling phenomena, especially when solidification stages are involved in the processes.[41] Caking by denatured and/or crystallized protein and consequent plugging of the membrane pores could be a detrimental effect when large-scale crystallization operations would be realized. The hydrophobic interaction between the protein molecules and the membrane surface could even enhance this effect.[42] For these reasons, the membrane performances have been evaluated by pure water flux measurements, by determining the volume reduction as a function of the time. In Figure 4 are shown the variations of pure water volumes, for the crystallization experiments operated with PPTAS. Water flux measurements were taken before the tests, between two consecutive experiments, at different values of solution velocity, and finally after the experiments. As clearly shown in the figure, no significant variation in solvent flux extraction was observed in the forced solution flow configuration, as all the observed volume variations are ~5% of the average values. This demonstrates that no losses in membrane performances, due to fouling and/or caking, have challenged the crystallization processes. Instead, a large amount of crystals have been grown on the membrane surface in the case of the static crystallization experiments. In Figure 5 is shown some portions of the membrane surface where trypsin crystals were grown in quiescent conditions.

These differences reside in the different mechanisms of the crystallization process between the two configurations. Low elapsed time for crystals' appearance and accelerated growth kinetics have already confirmed, in both configurations, the action of the membrane surface as a site for heterogeneous crystallization induced by

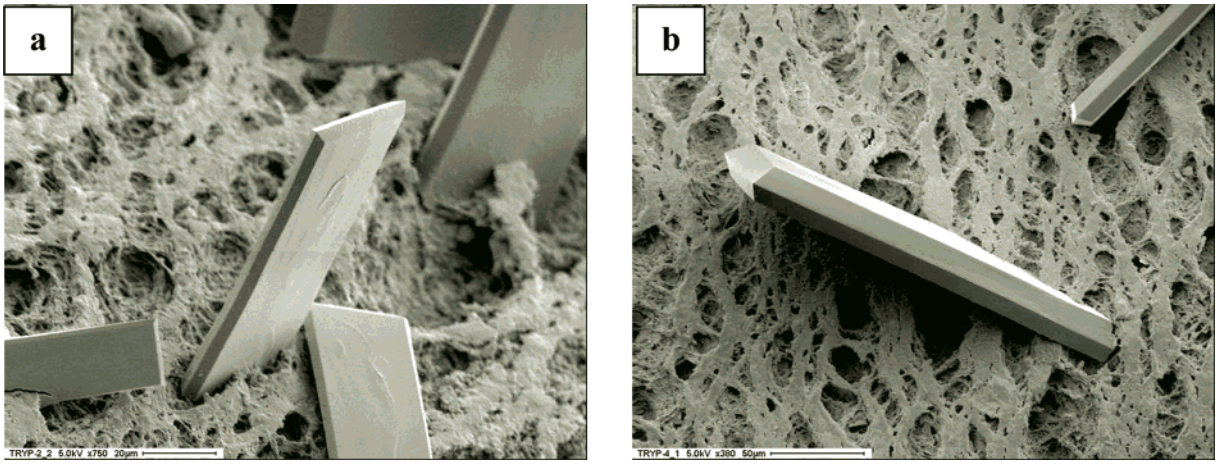

Figure 5. PPT crystals grown on the surface of the polymeric membrane, in static crystallization test.

Table 3. Apparent Yield of the PPTAS Crystallization Tests Carried out in Forced Solution Flow and Static Configurations

dynamic experiments		static experiments	
v (μm s^{-1})	yield (%)	m (no.)	yield (%)
557	91.9	1	93.9
932	93.6	2	92.0
1053	92.5	3	92.4
1170	92.8	4	92.6
1287	91.7	5	89.7
1524	92.3	6	89.7

local interactions with the protein macromolecules, thus promoting molecular collisions and formation of crystal nuclei susceptible of further growth.[24,25] If on one hand, in the static configuration, this mechanism induces the nucleation and the successive crystal growth in the same region of the membrane surface, thus producing the observed membrane surface covering, in the case of forced solution flow system a different mechanism appears to be the most reasonable. Protein crystals can, for example, nucleate at the surfaces of the membrane, grow to a certain stage, and move-off back into solution, because of the drainage force of the mass flow, leaving behind a new nucleation site. In this last case, no membrane caking is generated by the crystallization process.

Table 3 reports the apparent yields of the PPT crystallization tests. An interesting point is that only a slight reduction in the amount of protein crystallized (>90%) has been observed in dynamic experiments with respect to the static ones. This means that the possible loss of protein, caused by, for example, denaturation in the forced solution flow configuration or by interaction with the hydrophobic membrane surface, is quite limited in the range of the axial velocities investigated in this work.

Conclusions

The experimental results presented in this paper validate the effectiveness of the membrane crystallization technique for growing uniform enzyme crystals, with controlled morphological properties and high structural order and diffracting power.

Forced solution flow affects crystal growth kinetics, in the regime of the pronounced component of convective transport control in the overall process, in such a way that solute supply to the solid/liquid interface is enhanced by convection. The effect is the increase in crystal growth rate by increasing solution velocity up to a maximum, which depends, among other parameters, on the kinematic viscosity of the crystallizing solution. Once the maximum value is reached, the shifting of the operational working point from diffusive to interfacial kinetics in the overall process control leads to a decrease of growth rate, up to growth cessation. Although impurities perhaps have some effects on the process, in the membrane-based system mainly the excess of nucleation for extreme values of recirculating velocities seems to be responsible for growth deceleration, as demonstrated by the fact that low-purity level trypsin solutions have been favorably affected by convection up to a solution velocity of ca. 1500 μm/s. This represents an important improvement in view of lysozyme crystals being negatively affected by solution convection already at $v = 250$ μm/s, when using high-purity level solutions. In these conditions, the rate-limiting step of the growth process is the inclusion of the growing units from the boundary layer to the crystal surface. Hence, convection-enhanced protein concentrations lead to an excess of nucleation in the depletion zone and, therefore, to a crystal shower that suppresses growth. This means that, even with low-purity level solutions, by using the membrane system, protein crystals can be positively grown in forced solution flow configuration.

The hypothesis that the shift of the working conditions to a pure kinetic or transport control mechanism from a mixed condition, as in the case of the quiescent configuration, would result in a more steady growth has been confirmed by X-ray analysis, which demonstrated the excellent diffracting properties of the membrane-produced trypsin crystals.

Convection orients the growing crystals along the direction of the mass flow and affects crystal growth rate in a different manner with respect to specific crystal faces. Crystal shape is thus "tunable" using the membrane technique, by acting on the fluid-dynamic regime of the system: i.e., by operating on the solution velocity and/or on the kinematic viscosity of the solutions (e.g., by choosing an appropriate precipitating agent solution).

The trypsin crystals obtained demonstrated excellent features in terms of size uniformity. Values of CV, Span, and σ% are comparable or even better than those obtained in previous studies. Conversely to the static case, membrane performances are not challenged by

denatured and/or crystallized protein caking on the polymeric surface in dynamic configuration, thus indicating a possible positive application of this technique in large-scale production of enzymes in crystalline formulation, which is the case of CLECs.

Acknowledgment

Authors thank Dr. Mariano Davoli, Dipartimento di Scienze della Terra, Università della Calabria, for the SEM images.

Literature Cited

(1) McPherson, A. Introduction to protein crystallization. *Methods* **2004**, *34*, 254.

(2) Hui, R.; Edwards, A. High-throughput protein crystallization. *J. Struct. Biol.* **2003**, *142*, 154.

(3) Pechkova, E.; Nicolini, C. Protein nanocrystallography: A new approach to structural proteomics. *Trends Biotechnol.* **2004**, *22*, 117.

(4) Bodenstaff, E. R.; Hoedemaeker, F. J.; Kuil, M. E.; de Vrind, H. P. M.; Abrahams, J. P. The prospects of protein nanocrystallography. *Acta Crystallogr., Sect. D* **2002**, *58*, 1901.

(5) McPherson, A. *Crystallization of biological macromolecules*; Cold Spring Harbor Laboratory Press: Cold Spring Harbor, NY, 1999.

(6) Doye, J. P. K.; Louis, A. A.; Vendruscolo, M. Inhibition of protein crystallization by evolutionary negative design. *Phys. Biol.* **2004**, *1*, P9.

(7) Kirk, O.; Borchert, T. V.; Fuglsang, C. C. Industrial enzyme applications. *Curr. Opin. Biotechnol.* **2002**, *13*, 345.

(8) Schmid, A.; Hollmann, F.; Park, J. B.; Bühler, B. The use of enzymes in the chemical industry in Europe. *Curr. Opin. Biotechnol.* **2002**, *13*, 359.

(9) Vellard, M. The enzyme as drug: Application of enzymes as pharmaceuticals. *Curr. Opin. Biotechnol.* **2003**, *14*, 444.

(10) St. Clair, N. L.; Navia, M. A. Cross-linked enzyme crystals as robust biocatalysts. *J. Am. Chem.* Soc. **1992**, *114*, 7314−7316.

(11) Navia, M. A.; St Clair, N. Use of cross-linked crystals as a novel form of enzyme immobilization. Patent WO9202617, 1992.

(12) Margolin, A. L.; Khalaf, N. K.; St. Clair, N. L.; Rakestraw, S. L.; Shenoy, B. C. Stabilized protein crystals, formulations comprising them and methods of making them. Patent US2003175239, 2003.

(13) Margolin, A. L.; Navia, M. A. Protein crystals as novel catalytic materials. *Angew. Chem., Int. Ed.* **2001**, *40*, 2204.

(14) Roy, J. J.; Abraham, T. E. Strategies in Making Cross-Linked Enzyme Crystals. *Chem. Rev.* **2004**, *104*, 3705.

(15) Govardhan, C. P. Cross-linking of enzymes for improved stability and performance. *Curr. Opin. Biotechnol.* **1999**, *10*, 331.

(16) Vilenchik, L. Z.; Griffith, J. P.; St. Clair, N.; Navia, M. A.; Margolin, A. L. Protein Crystals as Novel Microporous Materials. *J. Am. Chem. Soc.* **1998**, *120*, 4290.

(17) Cvetkovic, A.; Picioreanu, C.; Straathof, A. J. J.; Krishna, R.; van der Wielen, L. A. M. Relation between Pore Sizes of Protein Crystals and Anisotropic Solute Diffusivities. *J. Am. Chem. Soc.* **2005**, *127*, 875.

(18) Falkner, J. C.; Al-Somali, A. M.; Jamison, J. A.; Zhang, J.; Adrianse, S. L.; Simpson, R. L.; Calabretta, M. K.; Radding, W.; Philips, G. N.; Colvin, V. L. Generation of Size-Controlled, Submicrometer Protein Crystals. *Chem. Mater.* **2005**, *17*, 2679.

(19) Vuolanto, A.; Uoitila, S.; Leisola, M.; Visuri, K. Solubility and crystallization of xylose isomerase from *Streptomyces rubiginosus*. *J. Cryst. Growth* **2003**, *257*, 403.

(20) Bakker, W. J. W.; Geertman, R. M.; Reedijk, M. F.; Baltussen, J. J. M.; Bargeman, G.; van Lare, C. E. J. Antisolvent solidification process. Patent WO2004096405, 2004.

(21) Drioli, E.; Curcio, E.; Di Profio, G. State of the art and recent progresses in membrane contactors. *Chem. Eng. Res. Des.* **2005**, *83*, 223.

(22) Curcio, E.; Di Profio, G.; Drioli, E. Membrane crystallization of macromolecular solutions. *Desalination* **2002**, *145*, 173.

(23) Curcio, E.; Di Profio, G.; Drioli, E. A new membrane-based crystallization technique: Tests on lysozyme. *J. Cryst. Growth* **2003**, *247*, 166.

(24) Di Profio, G.; Curcio, E.; Cassetta, A.; Lamba, D.; Drioli, E. Membrane crystallization of lysozyme: Kinetic aspects. *J. Cryst. Growth* **2003**, *257*, 359.

(25) Di Profio, G.; Curcio, E.; Drioli, E. Trypsin crystallization by membrane-based techniques. *J. Struct. Biol.* **2005**, *150*, 41.

(26) Curcio, E.; Simone, S.; Di Profio, G.; Drioli, E.; Cassetta, A.; Lamba, D. Membrane crystallization of lysozyme under forced solution flow. *J. Membr. Sci.* **2005**, *257*, 134.

(27) Pusey, M.; Witherow, W.; Naumann, R. Preliminary investigations into solutal flow about growing tetragonal lysozyme crystals. *J. Cryst. Growth* **1988**, *90*, 105.

(28) Pusey, M. L. Continuing adventures in lysozyme crystal growth. *J. Cryst. Growth* **1992**, *122*, 1.

(29) Nyce, T. A.; Rosenberger, F. Growth of protein crystals suspended in a closed loop thermosyphon. *J. Cryst. Growth* **1991**, *110*, 52.

(30) Miller, T. Y.; He, X.; Carter, D. C. A comparison between protein crystals grown with vapor diffusion methods in microgravity and protein crystals using a gel liquid−liquid diffusion ground-based method. *J. Cryst. Growth* **1992**, *122*, 306.

(31) DeLucas, L. J.; Moore, K. M.; Long, M. M.; Rouleau, R.; Bray, T.; Crysel, W.; Weise, L. Protein crystal growth in space, past and future. *J. Cryst. Growth* **2002**, *237*−*239*, 1646.

(32) Beth, M.; Broom, M. B. H.; Witherow, W. K.; Snyder, R. S.; Carter, D. C. Preliminary observations of the effect of solutal convection on crystal morphology. *J. Cryst. Growth* **1988**, *90*, 130.

(33) Vekilov, P. G.; Rosenberger, F. Protein crystal growth under forced solution flow: Experimental setup and general response of lysozyme. *J. Cryst. Growth* **1998**, *186*, 251.

(34) Adachi, H.; Takano, K.; Matsumura, H.; Inoue, T.; Mori, Y.; Sasaki, T. Protein crystal growth with a two-liquid system and stirring solution. *J. Synchrotron Radiat.* **2004**, *11*, 121.

(35) Adachi, A.; Matsumura, H.; Takano, K.; Nino, A.; Inoue, T.; Yoshimura, M.; Mori, Y.; Sasaki, T. New Practical Technique for Protein Crystallization with Floating and Stirring Methods. *Jpn. J. Appl. Phys.* **2003**, *42*, L1161.

(36) Kadowaki, A.; Yoshizaki, I.; Rong, L.; Komatsu, H.; Odawara, O.; Yoda, S. Improvement of protein crystal quality by forced flow solution. *J. Synchrotron Radiat.* **2004**, *11*, 38.

(37) Lin, H.; Rosenberger, F.; Alexander, J. I. D.; Nadarajah, A. Convective−diffusive transport in protein crystal growth. *J. Cryst. Growth* **1995**, *151*, 153.

(38) Vekilov, P. G.; Alexander, J. I. D.; Rosenberger, F. Nonlinear response of layer growth dynamics in the mixed kinetics−bulk-transport regime. *Phys. Rev. E* **1996**, *54*, 6650.

(39) Dirksen, J. A.; Ring, T. A. Fundamentals of crystallization: Kinetic effects on particle size distributions and morphology. *Chem. Eng. Sci.* **1991**, *46*, 2389.

(40) McPherson, A. Effects of a Microgravity Environment on the Crystallization of Biological Macromolecules. *Microgravity Sci. Technol.* **1993**, *6*, 101.

(41) Kang, S.-T.; Subramani, A.; Hoek, E. M. V.; Deshusses, M. A.; Matsumoto, M. R. Direct observation of biofouling in cross-flow microfiltration: Mechanisms of deposition and release. *J. Membr. Sci.* **2004**, *244*, 151.

(42) Chan, R.; Chen, V. Characterization of protein fouling on membranes: Opportunities and challenges. *J. Membr. Sci.* **2004**, *242*, 169.

Received for review July 13, 2005
Revised manuscript received September 23, 2005
Accepted September 27, 2005

IE0508233